Technical University of Denmark

DTU

Modelling of CMUTs with Anisotropic Plates

la Cour, Mette Funding; Christiansen, Thomas Lehrmann; Jensen, Jørgen Arendt; Thomsen, Erik Vilain

[Link back to DTU Orbit](#)

DTU Library
Technical Information Center of Denmark

Modelling of CMUTs with Anisotropic Plates

Mette Funding la Cour*†, Thomas Lehrmann Christiansen†, Jørgen Arendt Jensen* and Erik V. Thomsen†

*Center for Fast Ultrasound Imaging, Department of Electrical Engineering, Technical University of Denmark,
DK-2800 Kgs. Lyngby, Denmark

†Department of Micro and Nanotechnology, Technical University of Denmark, DK-2800 Kgs. Lyngby, Denmark

Abstract—Traditionally, CMUTs are modelled using the isotropic plate equation and this leads to deviations between analytical calculations and FEM simulations. In this paper, the deflection profile and material parameters are calculated using the anisotropic plate equation. It is shown that the anisotropic calculations match perfectly with FEM while an isotropic approach causes up to 10% deviations in deflection profile. Furthermore, we show how commonly used analytic modelling methods such as static calculations of the pull-in voltage and dynamic modelling through an equivalent circuit representation can be adjusted to include the correct anisotropic behaviour by using an effective flexural rigidity. The anisotropic caluclations are also compared to experimental data from actual CMUTs showing an error of maximum 3%.

I. Introduction

Capacitive micromachined ultrasonic transducers (CMUT) are a promising alternative to piezoelectric transducers and receive considerable attention due to their advantages such as wider bandwidth, higher sensitivity, ease of array fabrication and integration [1], [2]. Analytical and finite element calculations are important for efficient design of CMUTs and much has been put into modelling the behavior of the CMUT using mostly lumped element calculations [1] or finite element modelling [3]. Currently, the analytical approach to modelling the CMUT is based on the isotropic plate equation from which the deflection profile $w(x, y)$ can be obtained.

With the fusion bonding fabrication technology [4], the plate usually consists of crystalline silicon which is an anisotropic material. This leads to differences between analytical deflection profiles calculated with the isotropic plate equation and deflection profiles calculated by finite element programs that uses the correct anisotropic approach.

In this paper, the performance of CMUTs will be analytically calculated using the correct anisotropic approach. Utilising the anisotropic plate equation with fixed boundary conditions, the exact solution for the deflection profile can be obtained. The anisotropic solution is compared to the isotropic solution and FEM simulations. By combining the isotropic and anisotropic deflection profiles an effective flexural rigidity can be found. Using this, the pull in condition is found for a generalised case through energy considerations and the resonance frequency is found by lumped element modelling and compared to measurements. The objective is thus to show that using the anisotropic plate equation gives results matching FEM simulations and to demonstrate how this can easily be implemented into commonly used methods for calculating the performance of CMUTs.

II. The isotropic plate equation

In some cases, the CMUT devices have a thin plate made of an isotropic material, such as silicon nitride, and the static deflection profile, $w(x, y)$, is calculated by solving the isotropic plate equation [5]

$$\frac{\partial^4 w}{\partial x^4} + 2\frac{\partial^4 w}{\partial x^2 \partial y^2} + \frac{\partial^4 w}{\partial y^4} = \frac{p}{D_i} \tag{1}$$

where p is the applied pressure difference across the plate and the flexural rigidity is given by

$$D_i = \frac{E}{12\left(1 - \nu^2\right)}h^3 \tag{2}$$

where E is the Young's modulus, ν is the Poisson's ratio, and h is the thickness of the plate. The plate equation is then solved using appropriate boundary conditions.

The plate material, however, is not always isotropic. Crystalline silicon is an anisotropic material with a diamond cubic crystal structure. For plates made on silicon (111) substrates, Young's modulus and Poisson's ratio are constant and the isotropic plate equation can be used. However, for other silicon substrates, such as silicon (001) and silicon (011), Young's modulus and Poisson's ratio are strongly anisotropic, and (1) and (2) are therefore no longer valid.

III. The anisotropic plate equation

The differential equation for the deflection, $w(x, y)$, of a thin, anisotropic plate exposed to a uniform load p is [6]

$$\frac{\partial^4 w}{\partial x^4} + k_1\frac{\partial^4 w}{\partial x^3 \partial y} + k_2\frac{\partial^4 w}{\partial x^2 \partial y^2} + k_3\frac{\partial^4 w}{\partial x \partial y^3} + k_4\frac{\partial^4 w}{\partial y^4} = \frac{p}{D_h} \tag{3}$$

where

$$k_1 = \frac{4\hat{c}_{16}}{\hat{c}_{11}} \quad k_2 = \frac{2(\hat{c}_{12}+2\hat{c}_{66})}{\hat{c}_{11}} \quad k_3 = \frac{4\hat{c}_{26}}{\hat{c}_{11}}$$
$$k_4 = \frac{\hat{c}_{22}}{\hat{c}_{11}} \quad D_h = \frac{1}{12}h^3\hat{c}_{11} \tag{4}$$

and $\hat{c}_{pq}$ are the elements of the reduced stiffness tensor in the plate coordinate system (using the engineering strain convention) given by [6]

$$\hat{c}_{pq} = c'_{pq} - \frac{c'_{p3}c'_{3q}}{c'_{33}} \tag{5}$$

Here, c'_{ij} are the elements of the stiffness tensor in the plate coordinate system.

By aligning the plate coordinate system to the crystallographic coordinate system the expressions in (4) can be

c_{11}	c_{12}	c_{44}
165.6 GPa	63.9 GPa	79.5 GPa
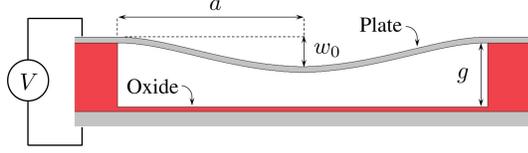
Fig. 1. Cross sectional view of CMUT cell with applied voltage.

Fig. 2. Normalised deflection profile of a thin circular plate of silicon (001) as calculated by (10), (12), (11) and FEM. The anisotropic profile is on top of the FEM simulations.
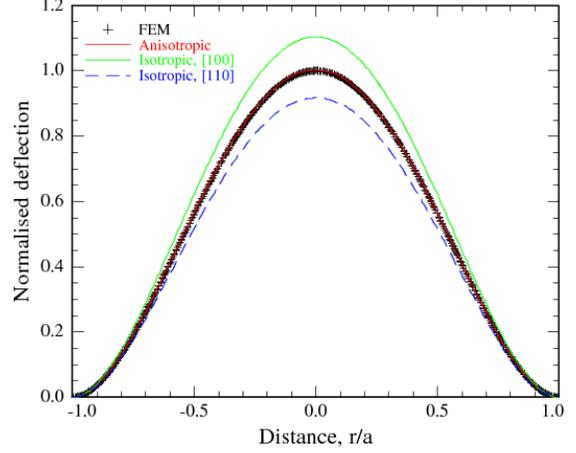
expressed through the stiffness coefficients of silicon shown in Table I [7].

For a thin circular plate on a (100) substrate, we obtain

$$k_1 = k_3 = 0 \tag{6}$$

$$k_2 = \frac{2c_{12}}{c_{11} + c_{12}} + \frac{4c_{11}c_{44}}{c_{11}^2 - c_{12}^2} = 2.81 \tag{7}$$

$$k_4 = 1 \tag{8}$$

$$D_h = \frac{1}{12}\left(c_{11} - \frac{c_{12}^2}{c_{11}}\right)h^3 = 11.75 \text{ GPa} \cdot h^3 \tag{9}$$

The solution to (3) for a circular plate of radius a fixed at the boundary is easily obtained using polar coordinates. The deflection at a point a distance r from the center is given by [5]

$$w(r) = w_0\left(1 - \left(\frac{r}{a}\right)^2\right)^2 \tag{10}$$

This equation is similar to the deflection profile for the isotropic case, however, the center deflections are different

$$w_{0,\text{isotropic}} = \frac{1}{64}\frac{a^4 p}{D_i} \tag{11}$$

$$w_{0,\text{anisotropic}} = \frac{1}{8(3 + k_2 + 3k_4)}\frac{a^4 p}{D_h} \tag{12}$$

Fig. 1 shows a cross sectional view of a CMUT cell with an applied voltage with parameters shown.

By equating (11) and (12) and isolating D_i it is possible to find an effective flexural rigidity

$$D_{\text{eff}} = \frac{3 + k_2 + 3k_4}{8}D_h \tag{13}$$

This can be used to change from the isotropic equation to the anisotropic equation in commonly used analytical models of CMUTs. Examples of this will be shown in the following sections.

Fig. 2 shows the normalised deflection profiles, using (10) to (12), of a CMUT exposed to a pressure difference. Using Young's modulus and Poisson's ratio along the [100] direction (E_{100}=130 GPa, ν_{100}=0.278) gives the solid green curve and using Young's modulus and Poisson's ratio along the [110] direction (E_{110}=169 GPa, ν_{110}=0.062) gives the dashed blue curve. The anisotropic solution is shown as a dotted red curve

and is on top of the FEM simulation shown for comparison. The FEM simulations were performed in COMSOL 4.2a using the full anisotropic stiffness tensor. Excellent agreement between the anisotropic solution and the finite element calculation is seen. The figure also shows that Young's modulus and Poisson's ratio corresponding to [100] or [110] directions leads to errors in the center deflection of around 10%. To reduce this error, it is common practice to use mean values of Young's modulus and Poission's ratio (E_{ave}=148 GPa, ν_{ave}=0.177) which decreases the error to around 1.5%. However, using the anisotropic approach gives the exact result. The error between the anisotropic calculation and FEM is less than 0.3%.

IV. ANALYTICAL MODELLING

As mentioned previously, the behavior of CMUTs are in most cases modelled using lumped element analysis or finite element analysis. In the following, an analytical model for CMUTs based on energy and force considerations will be presented. By investigating the energies of the system it is possible to estimate pull-in voltage and distance [8]. This approach also applies when using the anisotropic plate equation and an example will be given in the end of the section.

The total potential energy of the plate, U_t, has three terms

$$U_t = U_p + U_e + U_s \tag{14}$$

where U_p is the energy associated with pressure, U_e is the electrostatic energy due to the capacitor and U_s is the strain energy stored in the deflected plate. Equation (10) is the solution to the plate equation when a uniform pressure is applied. The electrostatic pressure is not uniform but as observed by [8] it is a very good approximation.

The energy contribution from the pressure difference is calculated as the work performed (i.e. force times length, here pressure times area times length) when deflecting the plate

$$U_p = -\int_0^a 2\pi p r w\, dr = -\frac{1}{3}a^2 p\pi w_0 \tag{15}$$

The electrostatic energy for an applied voltage V is given by

$$U_{\mathrm{e}} = -\frac{1}{2} C_{\mathrm{t}} V^2 \tag{16}$$

where the total capacitance C_{t} is given from the capacitance of the plate C_{pl} and of the insulating oxide C_{ox}

The potential energy associated with the plate acting as a spring is given by

$$U_{\mathrm{s}} = \frac{1}{2} D_{\mathrm{eff}} \int_0^a \left(\frac{\partial_r (r \partial_r w)}{r} \right)^2 2\pi r \, dr = \frac{32 D_{\mathrm{eff}} \pi w_0^2}{3a^2} \tag{17}$$

The flexural rigidity appears in this equation, making it possible to switch between isotropic and anisotropic cases.

By taking the derivative of the total potential energy with respect to the center deflection, the total equivalent force on the center of the plate can be found

$$F_{\mathrm{t}} = -\frac{\partial U_{\mathrm{t}}}{\partial w_0} = \frac{1}{3} a^2 p \pi - \frac{64 D_{\mathrm{eff}} \pi w_0}{3a^2} +$$

$$\frac{C_0 C_{\mathrm{ox}}^2 \sqrt{g} V^2 \left(\sqrt{g} w_0 + \sqrt{w_0} (-g + w_0) \operatorname{ArcTanh}\left[\sqrt{\frac{w_0}{g}} \right] \right)}{4 (g - w_0) w_0^2 \left(C_{\mathrm{ox}} + C_0 \sqrt{\frac{g}{w_0}} \operatorname{ArcTanh}\left[\sqrt{\frac{w_0}{g}} \right] \right)^2} \tag{18}$$

where g is the gap distance. The stable position of the plate is found when $F_{\mathrm{t}} = 0$. Thus, this equation can in principle be solved numerically to obtain the center deflection w_0 for a given design (C_0, g, a, D_{eff}) and operating conditions (V and p).

V. PULL IN VOLTAGE

To simplify the calculation, we normalise by using the following expressions

$$x_{00} = \frac{pa^4}{64 g D_{\mathrm{eff}}}, x_0 = \frac{g}{w_0}, k_{\mathrm{ox}} = \frac{C_0}{C_{\mathrm{ox}}}, V_{\mathrm{A}}^2 = V^2 \frac{3a^2 C_0}{256 D_{\mathrm{eff}} g^2 \pi} \tag{19}$$

x_{00} is the normalised deflection due to the external pressure, x_0 is the normalised center deflection, k_{ox} is the ratio of capacitances at zero voltage and V_{A} is the normalised applied voltage. This way (18) becomes

$$F_{\mathrm{tn}} = -x_0 + x_{00} -$$

$$\frac{V_{\mathrm{A}}^2 \left(\sqrt{x_0} + (-1 + x_0) \operatorname{ArcTanh}\left[\sqrt{x_0} \right] \right)}{(-1 + x_0) \sqrt{x_0} \left(\sqrt{x_0} + k_{\mathrm{ox}} \operatorname{ArcTanh}\left[\sqrt{x_0} \right] \right)^2} \tag{20}$$

The pull in voltage V_{PI} and the pull in point x_{PI} of the CMUT cell can be found from the expression of the force as $\partial F_{\mathrm{tn}}/\partial x_0 = 0$ and $F_{\mathrm{tn}} = 0$ apply. By isolating V_{A} in the first equation and substituting this result into the second, x_{PI} can be obtained and then afterwards V_{PI}.

For the special case where both the oxide thickness and the applied pressure is zero, the pull in distance becomes $x_{\mathrm{PI}} = 0.46$. For a parallel plate capacitor, this distance is

TABLE II
PULL IN VOLTAGES AND RESONANCE FREQUENCIES FOR THE SPECIAL CASE OF ZERO APPLIED PRESSURE AND ZERO OXIDE THICKNESS.

	V_{PI}	ω_0 (0 V)
Anisotropic	179 V	9.6 MHz
Isotropic [001]	172 V	9.1 MHz
Isotropic [011]	188 V	10.0 MHZ
Isotropic average	179 V	9.5 MHz

$x_{\mathrm{PI,parallel}} = 1/3$. With the corrected pull in distance, the pull in voltage becomes

$$V_{\mathrm{PI}} = \sqrt{\frac{89.4459 D_{\mathrm{eff}} g^2}{a^2 C_0}} \tag{21}$$

To compare calculations using the isotropic and anisotropic approaches, the pull in voltage for the special case (21) is found and shown in Table II. The calculation is performed with $a = 20$ μm, $h = 1$ μm and $g = 0.5$ μm. A difference of more than 10 V is observed so using different parameters for the calculations can make a considerable difference in the expected pull in voltage. Using the average values for Young's modulus and Poisson's ratio gives a result close to the correct anisotropic result.

VI. RESONANCE FREQUENCY

When modelling the dynamic behaviour of transducers, such as CMUTs, it is common practice to set up a lumped parameter equivalent circuit representation [9], [10], [11], [1]. Using the center displacement of the CMUT plate, w_0, and the equivalent charge on the plate, Q, as state variables, the state equations of the system are given by (18) and the three relations $V = Q/C_{\mathrm{t}}$, $i = dQ/dt$ and $v = dw_0/dt$. The system can then be linearized around a bias point $(w_{0,\mathrm{b}}, Q_{\mathrm{b}})$ by using the Jacobian of the system [11], [9], [10]

$$\begin{bmatrix} dV \\ dF_{\mathrm{t}} \end{bmatrix} = \begin{bmatrix} \left. \frac{\partial V}{\partial Q} \right|_{w_{0,\mathrm{b}},Q_{\mathrm{b}}} & \left. \frac{\partial V}{\partial w_0} \right|_{w_{0,\mathrm{b}},Q_{\mathrm{b}}} \\ \left. \frac{\partial F_{\mathrm{t}}}{\partial Q} \right|_{w_{0,\mathrm{b}},Q_{\mathrm{b}}} & \left. \frac{\partial F_{\mathrm{t}}}{\partial w_0} \right|_{w_{0,\mathrm{b}},Q_{\mathrm{b}}} \end{bmatrix} \begin{bmatrix} dQ \\ dw_0 \end{bmatrix} \tag{22}$$

The linearized system can then be transformed into the complex frequency domain by Lapace transform. Denoting the matrix in (22) as A, we get the following in the frequency domain

$$\begin{bmatrix} dV \\ dF_{\mathrm{t}} \end{bmatrix} = A \begin{bmatrix} dQ \\ dw_0 \end{bmatrix} = A \begin{bmatrix} \frac{1}{s} di \\ \frac{1}{s} dv \end{bmatrix} = B \begin{bmatrix} di \\ dv \end{bmatrix} \tag{23}$$

The lumped system components, the transformer factor and the coupling coefficient of the transducer can then easily be extracted from the matrix B [11]. The effective mass of the plate is attached to the terminals of the mechanical domain to complete the equivalent circuit as shown in Fig. 3, where k^* is the spring constant including spring softening. The effective mass is found through the relation $m_{\mathrm{eff}} = k_{\mathrm{eff}}/\omega_0^2$, where $k_{\mathrm{eff}} = \partial^2 U_{\mathrm{s}}/\partial w_0^2$ and ω_0 is the fundamental resonance frequency of the plate. The effect on the resonance frequency of using different flexural rigidities is demonstrated in Table II. Note that the velocity of the system in this calculation is
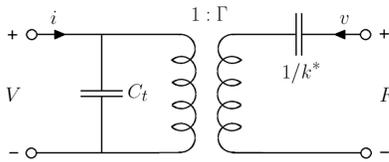
Fig. 3. Equivalent circuit diagram for a CMUT.

the velocity of the center of the plate. For correct coupling to the acoustic domain, a second transformer relation should be added to the equivalent circuit [9], [10]. Only the coupling between the electric and the mechanical domain is shown here for simplicity.

In such an equivalent circuit, the full anisotropic behaviour of the silicon plate is described by simply using the effective flexural rigidity as given in (13). This demonstrates that existing CMUT models can easily be accommodated to include the actual behaviour of single crystalline silicon plates.

VII. COMPARISON WITH MEASUREMENTS

To see how well the analytical model describes the behavior of CMUTs, measurements have been performed on fabricated devices. The impedance was measured with a HP 8752A network analyzer for varying bias voltages and the resonance frequency was found from the phase. The measurements were performed on two types of devices, half of them meant for phased array imaging with a frequency of 2.6 MHz ($a = 24.5$ μm, $h = 1.5$ μm, $g = 0.37$ μm and $t_{ox} = 0.21$ μm) and the others for linear array imaging with a frequency of 5 MHz ($a = 24.5$ μm, $h = 1.77$ μm, $g = 0.29$ μm and $t_{ox} = 0.21$ μm). Fig. 4 shows the resonance frequency as a function of applied voltage calculated for our two types of devices (red and green curve, circles). The corresponding analytical calculations are shown for comparison (blue and black curves, diamonds). Phased array device has solid curves and linear array device has dashed curves. The model is seen to match well with the measurements. The calculated values for the linear array device (dashed curves) has an average deviation from the measurements of $3\% \pm 0.7$ while for the phased array device (solid curves) it is only $2\% \pm 0.4$. The deviation can be explained by the metal electrode layer on top of the membrane causing a change in effective mass and flexural rigidity which is not included in the analytical calculations.

VIII. CONCLUSION

We have here demonstrated how wafer bonded CMUTs can be analytically modelled using the full anisotropic properties of single crystalline silicon. Using this approach, the analytic plate deflection profile shows excellent correspondence with FEM calculations. We have used a circular CMUT as an example to show how the anisotropic behaviour is easily incorporated into both static modelling of the pull-in voltage and dynamic equivalent circuit modelling by simply introducing an effective flexural rigidity. Using the anisotropic equivalent
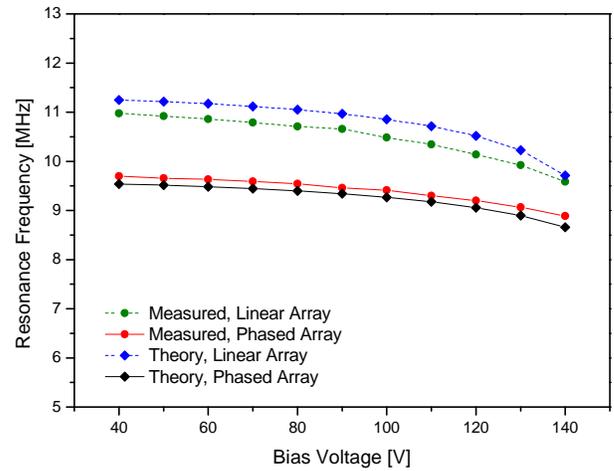

Fig. 4. Resonance frequency vs. applied voltage for measurement on two different devices and corresponding analytical curves.

circuit model, the resonance frequency as a function of bias voltage has been compared to measurements on wafer bonded CMUTs in order to evaluate the accuracy of the model.

REFERENCES

[1] I. Ladabaum, X. Jin, H. T. Soh, A. Atalar, and B. t. Khuri-Yakub, "Surface micromachined capacitive ultrasonic transducers," *IEEE Transactions on Ultrasonics, Ferroelectrics and Frequency Control*, vol. 45, no. 3, pp. 678–690, May 1998.

[2] O. Oralkan, A. Ergun, J. Johnson, M. Karaman, U. Demirci, K. Kaviani, T. Lee, and B. Khuri-Yakub, "Capacitive micromachined ultrasonic transducers: next-generation arrays for acoustic imaging?" *IEEE Transactions on Ultrasonics, Ferroelectrics and Frequency Control*, vol. 49, no. 11, pp. 1596 –1610, Nov. 2002.

[3] A. Lohfink, P.-C. Eccardt, W. Benecke, and H. Meixner, "Derivation of a 1D CMUT model from FEM results for linear and nonlinear equivalent circuit simulation," in *2003 IEEE Symposium on Ultrasonics*, vol. 1, Oct. 2003, pp. 465 – 468 Vol.1.

[4] Y. Huang, A. Ergun, E. Haeggstrom, M. Badi, and B. Khuri-Yakub, "Fabricating capacitive micromachined ultrasonic transducers with wafer-bonding technology," *Journal of Microelectromechanical Systems*, vol. 12, no. 2, pp. 128 – 137, Apr. 2003.

[5] S. Timoshenko and S. Woinowsky-Krieger, *Theory of Plates and Shells,*, 2nd ed. Mcgraw-Hill College, Jun. 1959.

[6] S. Holgate, "The transverse flexure of perforated aeolotropic plates," *Proceedings of the Royal Society A: Mathematical, Physical and Engineering Sciences*, vol. 185, no. 1000, pp. 50–69, Jan. 1946. [Online]. Available: http://adsabs.harvard.edu/abs/1946RSPSA.185...50H

[7] J. J. Hall, "Electronic effects in the elastic constants of n-type silicon," *Physical Review*, vol. 161, no. 3, pp. 756–761, Sep. 1967. [Online]. Available: http://link.aps.org/doi/10.1103/PhysRev.161.756

[8] H. Koymen, A. Atalar, E. Aydogdu, C. Kocabas, H. Oguz, S. Olcum, A. Ozgurluk, and A. Unlugedik, "An improved lumped element nonlinear circuit model for a circular CMUT cell," *IEEE transactions on ultrasonics, ferroelectrics, and frequency control*, vol. 59, no. 8, pp. 1791–1799, Aug. 2012, PMID: 22899125. [Online]. Available: http://www.ncbi.nlm.nih.gov/pubmed/22899125

[9] H. A. C. Tilmans, "Equivalent circuit representation of electromechanical transducers: I. lumped-parameter systems," *Journal of Micromechanics and Microengineering*, vol. 6, no. 1, pp. 157–176, Mar. 1996. [Online]. Available: http://iopscience.iop.org/0960-1317/6/1/036

[10] ——, "Equivalent circuit representation of electromechanical transducers: II. distributed-parameter systems," *Journal of Micromechanics and Microengineering*, vol. 7, no. 4, pp. 285–309, Dec. 1997. [Online]. Available: http://iopscience.iop.org/0960-1317/7/4/005

[11] S. D. Senturia, *Microsystem Design*. Springer, Nov. 2000.